

# Stabilizing amorphous calcium phosphate phase by citrate adsorption

Yan Chen,<sup>a,b</sup> Wenjia Gu,<sup>b</sup> Haihua Pan,<sup>\*a</sup> Shuqin Jiang,<sup>a,b</sup> Ruikang Tang<sup>a,b</sup>

<sup>a</sup>Qiushi Academy for Advanced Studies, Zhejiang University, Hangzhou 310027, China. E-mail: panhh@zju.edu.cn

<sup>b</sup>Department of Chemistry, and Centre for Biomaterials and Biopathways, Zhejiang University, Hangzhou 310027, China. E-mail: rtang@zju.edu.cn

## Experiments

### Materials:

All of the chemicals used in this study were of analytical grade and were purchased from Aladdin Reagent (Shanghai, China) unless specifically mentioned. Triple distilled water was used and all solutions were filtered through 0.22  $\mu\text{m}$  Millipore films prior to use.

### Crystallization kinetics:

Calcium solutions contained  $\text{CaCl}_2$  and  $\text{MgCl}_2$ , and phosphate solutions contained  $\text{Na}_2\text{HPO}_4$ ,  $\text{Na}_2\text{SO}_4$ ,  $\text{NaCl}$ ,  $\text{KCl}$ , N-2-hydroxyethylpiperazine-N'-2-ethanesulfonic acid, (HEPES, Genom BioMed Technology Inc., Hangzhou, China)<sup>S1</sup>. All experiments were conducted at temperature of  $37.0 \pm 0.5^\circ\text{C}$ . The SBF solutions were obtained by rapid mixing of equal volumes of designated calcium solutions and phosphate solutions, and the concentrations of each species in the final solution were list in Tables S1. To get solutions with  $\text{pH} 7.40 \pm 0.02$ , the  $\text{pH}$  of the initial phosphate solutions was pre-adjust to about 7.9 with  $1.0 \text{ mol L}^{-1}$   $\text{NaOH}$ . By try-and-error method, the calcium phosphate solutions with designated initial  $\text{pH}$  can be obtained. Sodium citrate was introduced either to phosphate solutions before mixing or to calcium phosphate solutions after mixing for about 10 min. The  $\text{pH}$  curve of each solution was monitored by a PHSJ-3F  $\text{pH}$  meter with E-201-C composite electrode (Leici Instrument, Shanghai, China). Each experiment has been repeated for at least four times (see Fig. S1 for reproducibility). The  $\text{pH}$  electrodes were calibrated by 25 mM  $\text{NaH}_2\text{PO}_4/\text{Na}_2\text{HPO}_4$  standard buffer solution ( $\text{pH} = 6.86$ ,  $25^\circ\text{C}$ ) and 10mM  $\text{Na}_2\text{B}_4\text{O}_7 \cdot 10\text{H}_2\text{O}$  standard buffer solution ( $\text{pH} = 9.18$ ,  $25^\circ\text{C}$ ) with an average error less than 0.02  $\text{pH}$  units. The induction times were determined by the intersections of tangents over the initially flat levels of  $\text{pH}$  (stage I) and over the subsequent fast  $\text{pH}$  drop during the precipitation of apatite (stage II) (cf. Fig. 1).

### Characterization:

At designated times, the suspension were removed and centrifuged at 10,000 g for 2 min (Eppendorf model 5418), and washed with ethanol for two times, and dried in vacuum for 24 h at  $40^\circ\text{C}$ . The mineral phase and crystallinity were characterized by FTIR (Shimadzu, IRAffinity-1) and XRD (Rigaku, Ultima IV with D/teX Ultra, Cu  $K\alpha$  radiation  $\lambda = 1.54 \text{ \AA}$ ). To get the citric acid concentration in minerals, the precipitate (about 2 mg) were dissolved in 2 mL hydrochloric acid solution ( $\text{pH}=1.5$ ), and analyzed by calibrated quantitative HPLC (WATERS 2690) with an ultraviolet-visible detector at 210 nm and an Ultimate AQ-C18 column (Welch Materials Inc. 250 mm  $\times$  4.6 mm, ID 5 $\mu\text{m}$ ). For TEM examination (Philips CM200 160kV; Hitachi HT-7700, 80kV), the samples were obtained by paddling copper grid in suspension, and washing with water and ethanol, and lamp-light dried. The zeta potentials of precipitate were determined by Zetasizer Nano S (Malvern). Calcium concentrations were determined by Chlorophosphonazo MA spectrophotometry<sup>S2</sup> and phosphate concentrations by phosphomolybdenum blue spectrophotometry<sup>S3</sup>.

### Solution Chemistry Calculation:

The supersaturations of the solutions were calculated by VMINTEQ 3.0.<sup>S4</sup> Davies approximation of the Debye–Hückel equation was used for calculating the activity coefficients (parameter  $b = 0.3$  is applied). The solubility product,  $K_{\text{SP}}$ , of HAP ( $\text{p}K_{\text{SP}} = 58.33$ , MINTEQ database: NIST 46.7), and ACP ( $\text{p}K_{\text{SP}} = 25.5$ <sup>S5, S6</sup>) were used in calculation.

## Notes and References

S1. HEPES act as a buffer reagent, which has been widely used in SBF solutions. HEPES can affect the nucleation kinetics of calcium phosphate. Control experiments are chosen to discount the effect of HEPES on nucleation. The difference in nucleation time can be considered as the effect of citrate on controlling nucleation.

S2. Q Xing-Chu, Z Yu-Sheng and Z Yin-Quan, *Analyst*, 1983, **108**, 754.

S3. L. Drummond and W. Maher, *Anal. Chim. Acta*, 1995, **302**, 69.

S4. J.P. Gustafsson, 2010. Visual MINTEQ, Version 3.0, Stockholm. Available from: <http://www.lwr.kth.se/English/OurSoftware/vminteq>.

S5. M. R. Christoffersen, J. Christoffersen, and W. Kibalczyk, *J. Cryst. Growth*, 1990, **106**, 349.

S6. As the morphology of ACP found in this work is analogues to that of ACP1 in ref S4,  $\text{p}K_{\text{SP}}=25.5$  is applied here.

## Tables

**Table S1.** The composition of simulated body fluid with initial pH 7.4 (adjusted with 1.0 M NaOH solution), ionic strength 0.15 M.

Ion.	Na <sup>+</sup>	K <sup>+</sup>	Mg <sup>2+</sup>	Cl <sup>-</sup>	SO <sub>4</sub> <sup>2-</sup>	Ca <sup>2+</sup>	HPO <sub>4</sub> <sup>2-</sup>	HEPES <sup>-</sup>
C/mM	130	5.0	1.5	135	0.5	8.0	4.8	10.0

**Table S2.** Concentrations and activities of calcium and phosphate ions in the presents and absents of citrate.

	[Ca <sup>2+</sup> ](mM)	[PO <sub>4</sub> <sup>3-</sup> ]	[Cit <sup>3-</sup> ]	{Ca <sup>2+</sup> }	{H <sub>x</sub> PO <sub>4</sub> <sup>y-</sup> } <sub>total</sub> <sup>*</sup>	Sat. Index (ACP) (log IAP-log K <sub>sp</sub> ) <sup>**</sup>	Sat. Index (HAP)
Control-1	8.0	4.8	0.0	6.4	2.5	1.91	14.0
Control-2	6.6	4.9	0.0	5.2	2.6	1.69	13.7
Cit-0	8.0	4.8	2.0	5.2	2.6	1.68	13.7

\* {H<sub>x</sub>PO<sub>4</sub><sup>y-</sup>}<sub>total</sub> = {PO<sub>4</sub><sup>3-</sup>} + {HPO<sub>4</sub><sup>2-</sup>} + {H<sub>2</sub>PO<sub>4</sub><sup>-</sup>} + {H<sub>3</sub>PO<sub>4</sub>}

\*\* IAP: ionic activity product; K<sub>sp</sub>: Solubility product

## Figures

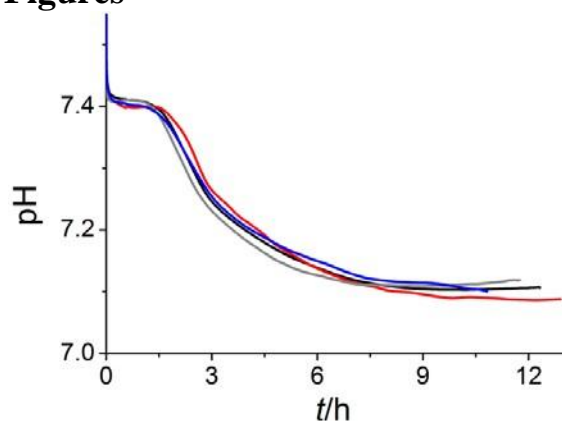


**Fig. S1** The reproducibility of pH curves.

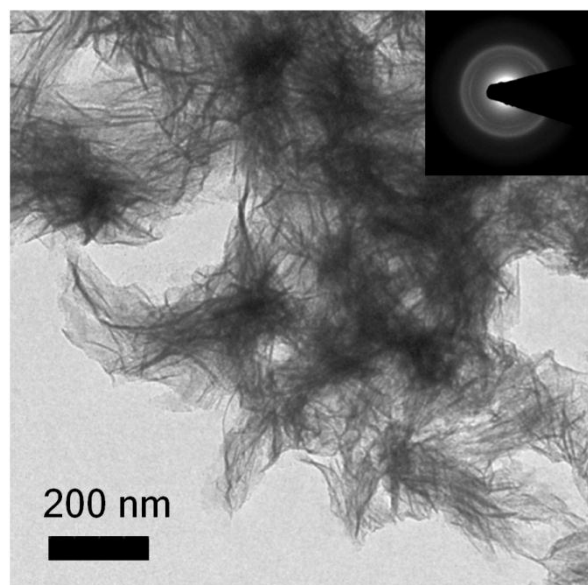


**Fig. S2** Sheet-like minerals were formed after crystallization.

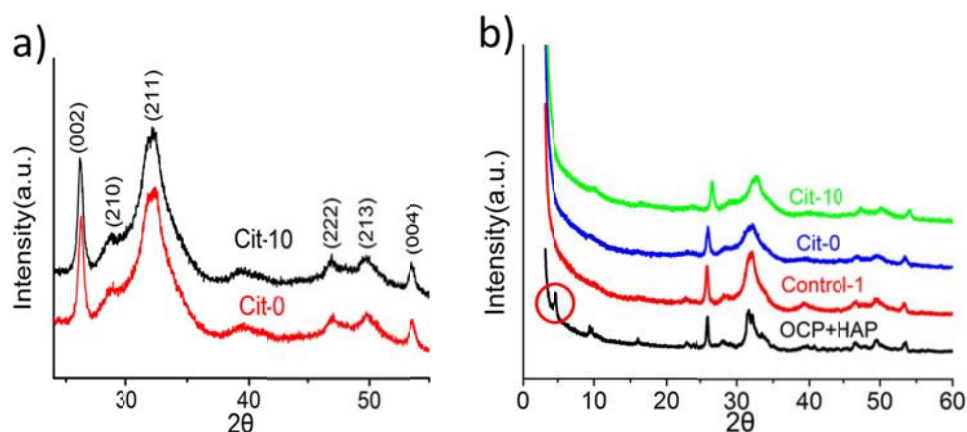


**Fig. S3** (a): XRD patterns of final crystallized minerals (at 10 hrs) in the presents of citrate. The XRD patterns match that of hydroxyapatite (JCPDS: 09-0432). (b): XRD patterns of initial crystallized minerals for different systems. The absence of diffraction peak at about 4.7 degree indicating the initial crystallized phase is HAP instead of OCP.

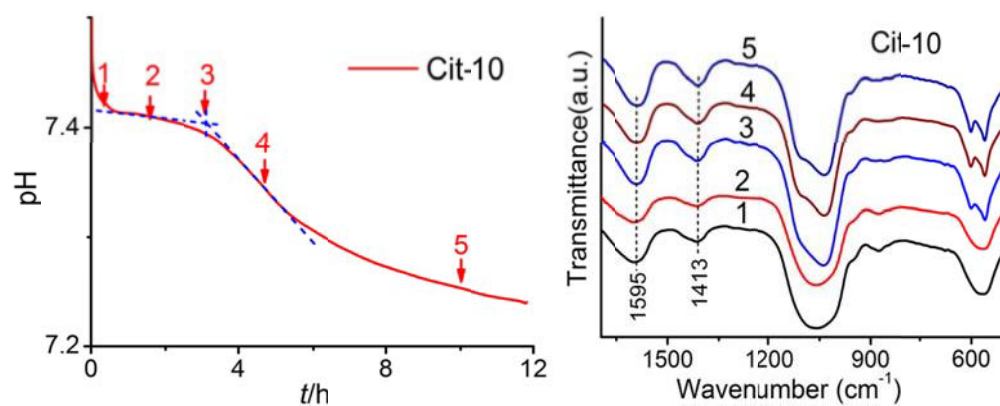


**Fig. S4** A representative pH curve (left) for Cit-10 system (introduce citrate after ACP formation for about 10min) and FTIR spectra (right) for the minerals during crystallization at designated times (marked in the pH curve on left).

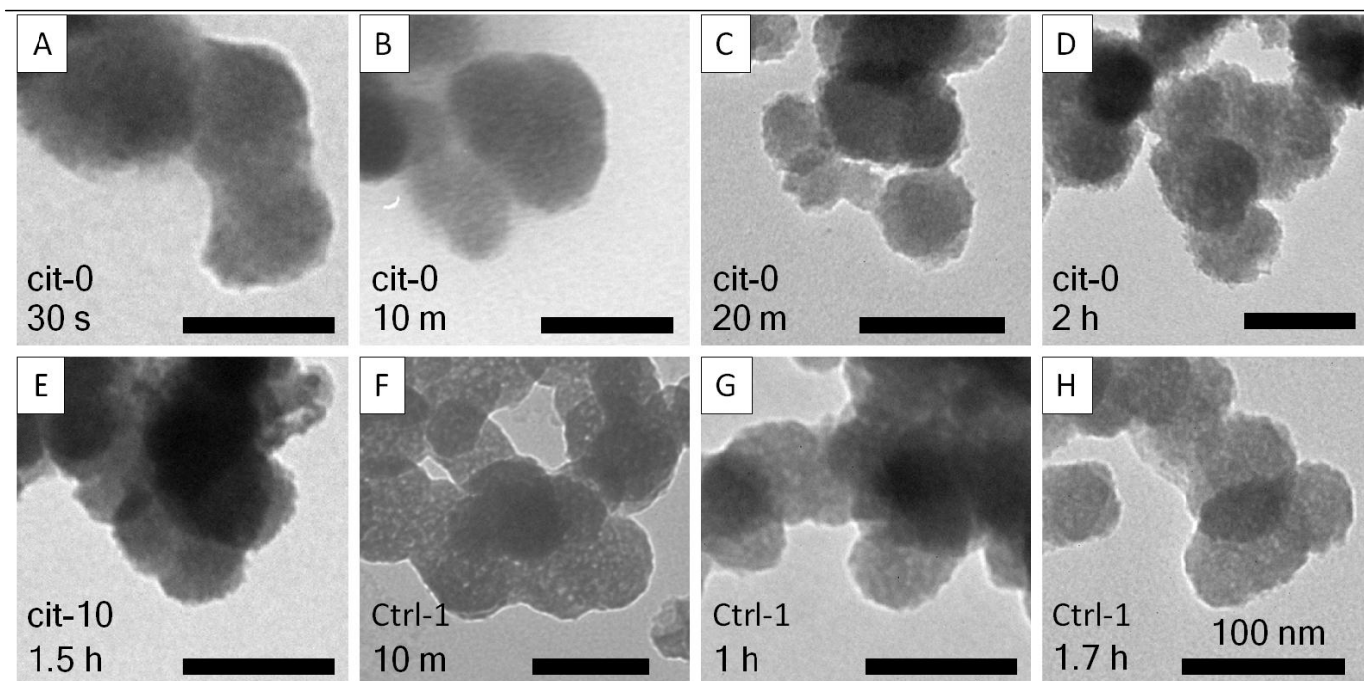


**Fig. S5** The morphology evolution of ACP particles. A-D: the surface of ACP particles become rougher in the present of citrate (cit-0 system). E: when citrate is introduced after ACP formation, it also become rougher. F-G: ACP surface is relative smooth in the absents of citrate before crystal nucleation (H, at induction time).

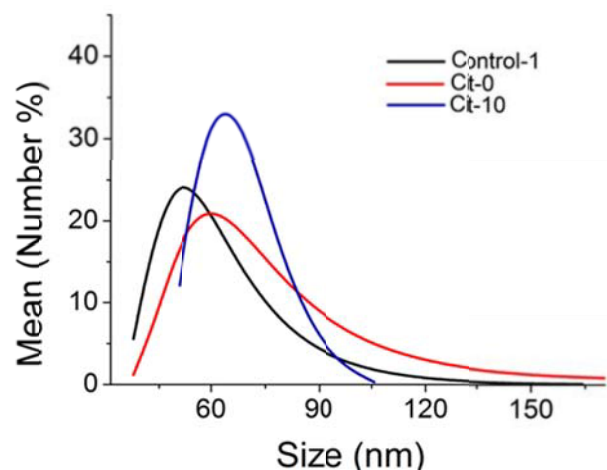


**Fig. S6** The particle size distributions of ACP particles.